Predicting Liquid-Liquid Phase Separation of Submicron Proxies for Atmospheric Secondary Aerosol

Qishen Huang[1,2], *Kiran R. Pitta*[2], *Andreas Zuend*[3], *Miriam Arak Freedman*[*, 2,4]

[1] Institute of Chemical Physics, School of Chemistry and Chemical Engineering, Beijing Institute of Technology, Beijing, 100081, China

[2] Department of Chemistry, The Pennsylvania State University, University Park, Pennsylvania 16802, United States

[3] Department of Atmospheric and Oceanic Sciences, McGill University, Montreal, Quebec, H3A 0B9, Canada

[4] Department of Meteorology and Atmospheric Science, The Pennsylvania State University, University Park, Pennsylvania 16802, United States

Abstract

Liquid–liquid phase separation (LLPS) of atmospheric aerosols can significantly impact climate, air quality, and human health. However, their complex composition, small size, and history-dependent properties result in great uncertainty in the modeling of aerosol phase state and atmospheric processes. Herein, using cryogenic transmission electron microscopy (cryo-TEM), we examined model submicron aerosols composed of organic compounds and ammonium sulfate, and established a parameterization for the separation relative humidity (SRH) that accounts for chemical composition, particle size, and equilibration time. We evaluated different variables that describe chemical composition: O/C ratio, partition coefficient, solubility, molar mass, and polarizability. The O/C ratio fits the SRH of micrometer droplets best, and by using a scaling factor to translate the micrometer SRH parameterization to submicron aerosols, we incorporate the effects of size and equilibration time. The measured scaling factor for the submicron mean SRH (30nm – 1μm, 20 min equilibration times) is 0.80, the factor becomes 1 with equilibration time over 1 hour, and is equal to 0, meaning that SRH is absent, when the aerosol dry diameter is smaller than 30 nm. Our parameterization will aid in universal SRH modeling, potentially leading to more accurate predictions of aerosol mass, optical properties, hygroscopicity, and heterogeneous chemistry.

Keywords: Liquid-liquid phase separation (LLPS), atmospheric secondary aerosols, submicron aerosol, separation relative humidity (SRH), O/C ratio.

Synopsis： This study provides a practical parameterization for liquid-liquid phase separation of atmospheric secondary aerosol particles, which accounts for aerosol chemical composition, size, and time evolution.

Introduction

Aerosol particles are ubiquitous in the atmosphere. They have significant effects on the Earth's climate via direct and indirect interactions, determine air quality via multiphase physics and chemistry, and impact public health via human exposure.[1–5] Atmospheric secondary aerosol particles, mainly composed of organic and inorganic compounds, is one of the most abundant species of the total aerosol loading. Field studies across the world show that organic compounds contribute to a large mass fraction of secondary aerosol particles (20-90 wt%).[6–8] The formation and evolution of atmospheric secondary aerosol particles involves various chemical and physical processes, and aerosol phase state is one of the key determining factors that dictates the role of secondary aerosol particles in the atmosphere.[9] Following changes in ambient relative humidity (RH), the aerosol water activity shifts, resulting in phase transition processes such as liquid–liquid phase separation (LLPS), homogeneous mixing mediated by water, efflorescence, and deliquescence.[3] LLPS of internally mixed organic/inorganic aerosol particles often occurs at relatively high RH, leading to separation into an organic-rich phase and an inorganic-rich phase, both with correspondingly high aerosol water activity (as imposed by the modified Raoult's law and, for submicron-sized particles, the Köhler equation, both of which take non-ideality into account).[10] Additionally, once LLPS occurs in organic—inorganic secondary aerosols, it often persists at least down to the efflorescence RH, the low RH levels where inorganic salts like ammonium sulfate crystallize. The occurrence of LLPS significantly changes aerosol mixing state and morphology, which can impact

gas–particle partitioning, heterogeneous chemistry, cloud condensation nuclei activity, and ice nucleation.[11]

Due to its complex composition, atmospheric secondary aerosol contributes a great amount of uncertainty to our understanding of Earth's climate and air quality. To the best of our knowledge, no measurement technique can thoroughly resolve the molecular composition of secondary aerosol particles; therefore, accurate prediction of LLPS based on representative variables is vital for understanding atmospheric processes and for improving atmospheric modeling. Much effort has been devoted to the prediction of the separation relative humidity (SRH) of LLPS, which refers to the RH at the occurrence of LLPS when dehydrating an aerosol from high RH. Using the oxygen-to-carbon ratio (O/C ratio) as the key variable, parameterizations have been established to predict the SRH.[12–14] The parameterizations were estimated by fitting to experimentally measured SRH values for secondary aerosol surrogates containing the sole inorganic compound of ammonium sulfate. Phase separation between organic species of different aqueous solubilities (e.g. primary and secondary organic aerosol) has also been reported recently, and the separation relative humidity between primary organic aerosol and secondary organic aerosol was also explained based on the O/C ratio.[15–17] Additionally, thermodynamic models can be used to predict the values of SRH as a function of aerosol composition. The Aerosol Inorganic–Organic Mixtures Functional groups Activity Coefficient model for nonideal mixing (AIOMFAC-LLE) can predict the water activity change and phase diagram of LLPS when molecular structure information about the system components is available.[18–22] However,

limitations exist for current parametrizations. First, experimentally established parameterizations for LLPS consider only the O/C ratio, and therefore overlook distinctions between different oxygen-containing functional groups. Second, the use of the thermodynamic model requires the exact composition of the system, which is not accessible from field-collected samples without resorting to assumptions.[23] Third, the effects of aerosol physicochemical properties, such as size, equilibration time, and aerosol pH, are not incorporated into the simple parameterization-based models.[24–29] In our recent work, we have shown a size effect on SRH using cryogenic transmission electron microscopy (cryo-TEM): the SRH in submicron SOA particles is suppressed or inhibited depending on their size.[28,30–32] We also found that the suppression of SRH in submicron aerosol particles is dependent on the equilibration time.[31,33]

Given these limitations, studies that can develop parameterizations for LLPS and SRH of submicron secondary aerosol particles will improve our understanding of the aerosol phase state by minimizing the uncertainty in the phase state prediction of atmospheric secondary aerosol. A proper parameterization for aerosol SRH should possess the following characteristics: i) accurately predict the presence of LLPS as well as the value of SRH with variables that can effectively represent the chemical composition of the organic component(s); ii) effectively reflect the effect of aerosol size and equilibration time; iii) have a simple form that can be easily incorporated into a large-scale atmospheric model. Considering the criteria, O/C ratio, molar mass, octanol–water partition coefficient (LogP, LogD, explained below), water solubility (LogS), and the polarizability of the organic component are potential variables that

depict different physicochemical properties of molecules. The O/C ratio is widely applied in atmospheric chemistry to roughly represent the degree of oxidation, the hygroscopicity, and as an influential factor on phase transition processes including LLPS.[34–37] Along with the O/C ratio, the molar mass of organic components has been investigated in a reduced-complexity thermodynamic model for organic-water binary systems.[38] LogP is defined as the logarithmically transformed partition coefficient between octanol and water (i.e., $\log_{10}(P)$; the same notation is used below for LogD and LogS), assuming the species of interest is neutral in charge. LogD is the octanol–water partition coefficient at a specific pH value. The LogS value represents the water solubility of the organic species. All LogP, LogD, and LogS values are estimated at room temperature (298 K). The polarizability of a molecule denotes the tendency of the molecule to develop an induced dipole moment subjected to an electric field. Polarizability can be particularly important when considering the interaction between neutral organic molecules and electrolytes.

In this study, we measured the SRH of various organic/inorganic mixtures for both micrometer droplets ($1 – 10^3$ μm in diameter) and submicron aerosol particles ($10 – 10^3$ nm in diameter). We established parameterizations for the presence of LLPS and the value of SRH for submicron organic/inorganic particles using two methods: i) numerical fits, including polynomial and sigmoidal fits, using a set of elected variables (O/C ratio, LogP and LogD, LogS, polarizability) and the measured SRH, ii) a scaling factor to predict the SRH for submicron aerosol particles using an established parameterization for the SRH of micrometer droplets, i.e. to capture the

influence of particle size in this regime. Regarding (i), we investigated these different parameterization variables and compared the results to a parameterization based only on the O/C ratio. Regarding (ii), we calculated scaling factors that effectively connect the SRH for micrometer droplets to the SRH for submicron aerosol particles with consideration of the size effect and equilibration time. Our results suggest that a scaling factor that accounts for the size and time effect on SRH of submicron aerosol particles combined with the parameterization as a function of chemical composition for micrometer droplets can result in an applicable prediction for LLPS of atmospheric secondary aerosol particles.

Materials and Methods

LLPS of micrometer droplets. For our study, we selected organic components with O/C ratios ranging from 0.33 to 0.67. The organic compounds used were 2-methylglutaric acid (2MGA, O/C = 0.67), 2,2-dimethylsuccinic acid (DMSA, O/C = 0.67), diethyl malonic acid (DEMA, O/C = 0.57), 3,3-dimethylglutaric acid (DMGA, O/C = 0.57), 2,5-dihydroxybenzoic acid (DHBA, O/C = 0.57), DL-4-hydroxy-3-methoxymandelic acid (HMMA, O/C = 0.56), PEG-400 (O/C = 0.56), 1,2,6-hexanetriol (O/C = 0.5) and 2,5-hexanediol (O/C = 0.33) (Table 1). Each organic component was mixed with ammonium sulfate (AS). The concentration of the solutions was 5 wt. %, containing organic and inorganic components in a 2:1 mass ratio, respectively, in high-performance liquid chromatography (HPLC) grade water. The mass ratio was chosen based on the typical mass fractions of organic and inorganic compounds for

atmospheric aerosol particles. In addition, the phase diagrams for SRH are usually flat (Figure S2) for a wide range of organic mass fractions, thus the 2:1 mass ratio is representative for the ternary mixture and a precise solute mass ratio is not that critical for the purpose of SRH predictions. Aerosol particles were generated by spraying the solution of interest onto hydrophobic glass slides. In the discussion, we will use the name or abbreviations of the organic compounds (Table 1) to refer to the aerosol composition, while all systems used are mixtures of an organic compound and AS.

The phase transitions of the aerosol particles were studied using a Nikon Eclipse Ti2 microscope, with a 20× objective. The size of the particles ranges from 20 μm – 200 μm in diameter. The hydrophobic slides were kept in a home-built environmental chamber. The relative humidity (RH) was controlled by mixing wet and dry nitrogen gas, and measured using a Vaisala HMP60 probe. Initially, the particles were dried at a rate of ~10% RH/second, until complete efflorescence was observed (<10% RH). Next, RH was increased at a uniform rate of 1% RH/min until deliquescence occurred. Once all the particles deliquesced, the particles were equilibrated for 20 minutes. After equilibration, RH was decreased at a uniform rate of 1% RH/min. Upon encountering a phase transition (LLPS and efflorescence) during the RH reduction, the rate of decrease of RH was reduced to approximately 0.5% RH/min. Images were collected at 5 min intervals. Reducing the rate at which the RH is changed allows us to observe the phase transitions of the aerosol particles. However, changing the dehumidification rate does not affect the SRH value of the systems studied.

Around 30 particles were characterized for every phase transition and the separation RH (SRH), efflorescence RH (ERH) and deliquescence RH (DRH) were determined for every particle (summarized in Table S1). For each system, the average SRH, ERH and DRH were determined based on all corresponding imaged particles.

Table 1. The separation relative humidity (SRH) measurement results achieved in this study. Aerosols are composed of the listed organic species and ammonium sulfate with an organic-to-inorganic dry mass ratio of 2:1.

Compound	O/C	Submicron SRH range	Submicron mean SRH	Micrometer SRH (Exp.)	Micrometer SRH (Ref.)
2-Methylglutaric acid (2MGA)	0.67	48-65%	59±4%	78.4±0.2%	75.3±2.8%[1]
2,2-Dimethylsuccinic acid (DMSA)	0.67	55-72%	66±6%	Not observed	Not observed[1]
Diethyl malonic acid (DEMA)	0.57	73-81%	77±4%	89.7±0.8%	89.2±3.0%[1]
3,3-Dimethylglutaric acid (DMGA)	0.57	74-83%	78±4%	89.2±2.1%	89.1±3.4%[1]
2,5-Dihydroxybenzoic acid (DHBA)	0.57	Not available	Not available	Not observed	Not observed[1]
DL-4-Hydroxy-3-methoxymandelic acid (HMMA)	0.56	48-74%	61±9%	73.1±1.0%	72.6±2.6%[1]
PEG-400	0.56	58-78%	70±7%	89.6±0.6%	88.0±1.0%[2]
1,2,6-Hexanetriol	0.5	50-71%	58±6%	74.03±0.1%	76.7±2.5%[1]
2,5-Hexanediol	0.33	52-78%	64±6%	87.7±1.5%	88.8±3.7%[1]

[1]You et al., Atmos. Chem. Phys. **2013**, 13 (23), 11723–11734.
[2]Song et al., Geophys. Res. Lett. **2012**, 39 (19), 1–5.

LLPS of submicron particles at different RH. The flash freeze technique coupled with transmission electron microscopy (TEM) was used to study the SRH of submicron

aerosol particles.[31,39] An aqueous solution of the organic and inorganic components was prepared in a 2:1 mass ratio at 0.05 wt.%. The composition of the aerosol particles used for the study were the same as for the optical microscopy experiments described above. Aerosol particles were generated using an atomizer (TSI 3076, TSI, Inc) and collected in a Tedlar bag (RH > 90%). The desired RH was obtained by injecting dry N_2 gas into the Tedlar bag. The particle number concentrations were measured via a condensation particle counter (CPC, TSI model 3752). The relative humidity was recorded using a combined RH and temperature probe (Vaisala HMP 110, ±1.5% RH). We set the RH using a binary search-like approach: first identifying the onset SRH and the final SRH, then setting intermediate RH values to determine the mean SRH. The mean SRH, represented by the average value and standard deviation, is calculated as the average RH of all phase-separated particles between the onset and final SRH. After obtaining the targeted RH, the particles were passed through a pre-cooled flow tube that is approximately 220K inside, maintained by chilled nitrogen gas.[39] The particles were vitrified at a high cooling rate (> 3×10^9 K/s) and collected on copper mesh grids cooled using dry ice.[31,39] These grids are carefully stored in liquid nitrogen. Cryo holders were precooled using liquid nitrogen in a cryo-station and the grid was transferred carefully into the precooled holders. Particles were imaged using a Tecnai LaB6 and FEI Talos Arctica G2 TEMs. A minimum of four experiments with different target RH levels were conducted for each solution. At each RH, 100-200 images of different particles were imaged and analyzed using Fiji software.

Parameterization of aerosol SRH. The estimation of the potential parameterization variables, LogP, LogD (at pH 7.4), and LogS, of the organic compounds were evaluated using the absorption, distribution, metabolism, excretion, and toxicity (ADMET) model: ADMETLab 2.0. The model uses the multi-task graph attention framework with the inclusion of 10370 molecules.[40] The input to the model is the simplified molecular-input line-entry system (SMILES) string characterizing the molecular structure of each organic species. The estimated polarizability was collected from the ChemSpider database (https://www.chemspider.com/). The estimated LogP, LogD, LogS, and polarizability values are listed in Table S2.

AIOMFAC-LLE modeling. The AIOMFAC-LLE model was applied to estimate the phase diagram and SRH for the systems of ammonium sulfate and the organic species in Table 1.[18–21] We calculated the phase diagrams of all organic/AS systems involved in this study for a temperature of 298 K to evaluate the effect of functional groups and their interactions with the inorganic ions and water on the phase diagram predicted from this thermodynamic model (Figure S2).

Results and Discussion

Parameterization of SRH for Micrometer Organic/AS Particles. We conducted optical microscopy measurements to characterize the SRH of micrometer aerosol particles. The measured SRH values agree with values reported in other published work, indicating the consistency of the SRH values across different studies for micrometer droplets (Table 1). Such consistency validates the accuracy of our

measurement protocol. Previous studies have provided parameterizations of SRH for micrometer SOA proxies. Based on the experimental data for the SRH of organic/AS particles, two parametrizations were reported:

i) Bertram et al.:[12]

$$\mathrm{SRH}(\%) = \begin{cases} 35.50 + 339.9 \times (\mathrm{O/C}) - 471.8 \times (\mathrm{O/C})^2, & 0.2 < \mathrm{O/C} < 0.7 \\ 0 & , 0.7 < \mathrm{O/C} < 1.4 \end{cases} \quad \text{(Eqn. 1)}$$

ii) Song et al.:[13]

$$\mathrm{SRH}(\%) = \begin{cases} \frac{10^{1.76}}{10^{1.76} + 0.11 \times 10^{3.45 \times (\mathrm{O/C})}} \times 100\%, & 0.0 < \mathrm{O/C} < 0.8 \\ 0 & , 0.8 < \mathrm{O/C} \end{cases} \quad \text{(Eqn. 2)}$$

Both parametrizations were constructed using datasets that cover numerous organic/inorganic mixture systems. However, the two parameterizations were based on different datasets. The parameterization from Bertram et al. were generated using second-order polynomial functions for ternary systems, which were composed of water, a single organic compound that varied from system to system, and AS. Song et al. fitted the data from Bertram et al. with the addition of several complex mixtures of up to ten organic species using a sigmoidal function. Additionally, further experimental data have been generated by Bertram and coworkers after these parametrizations were published.[14] Herein, we integrate all literature-reported SRH data for ternary systems (Figure 1).[12–14,41] The data for systems containing complex organic mixtures are not included since other candidate variables that will be investigated in this study are difficult to evaluate for complex organic mixtures. Detailed information about the dataset can be found in Table S3. We tested both a polynomial function (second order

polynomial function) and a sigmoidal function (four-parameter logistic function) for the parameterization (Figure 1a and 1b). Both the second-order polynomial fit and four parameter logistic fit indicated a threshold O/C ratio at 0.8, in agreement with Song et al. For the second-order polynomial fit, we set the lower bound of the O/C ratio for the polynomial fit as 0.2, since no experimental data have been reported for these low O/C values. The coefficient of determination (R^2) value is 0.62 (Figure 1a, red curve), improved from Bertram et al. (R^2 is 0.15 for the expanded dataset shown here, Figure 1a, black curve). The updated parameterization is as follows:

$$\mathrm{SRH}(\%) = \begin{cases} 17.8 + 369.4 \times (\mathrm{O/C}) - 431.1 \times (\mathrm{O/C})^2, & 0.2 < \mathrm{O/C} < 0.8 \\ 0 & , 0.8 < \mathrm{O/C} \end{cases} \quad \text{(Eqn. 3)}$$

For the sigmoidal fit, we applied the four-parameter logistic model with and without the robust fitting (Figure 1b). The four-parameter logistic fit (4PL) without robust fitting also has a R^2 value of 0.62. The four-parameter logistic fit with the least absolute residuals (4PL-LAR) robust fitting method better depicts the threshold value (the O/C value that differentiates LLPS from homogeneous particles) with a higher R^2 value of 0.85. Both 4PL and 4PL-LAR fits are improved compared to the parameterization by Song et al., which returns a R^2 value of 0.49 for the combined ternary system data (Figure 1b, grey curve). As the 4PL-LAR method provides a more accurate threshold O/C value for LLPS, we elect the 4PL-LAR fit as a more credible result:

$$\mathrm{SRH}(\%) = \begin{cases} 94.11 + \frac{-94.24}{1+(1.47(\mathrm{O/C}))^{-16.84}} & , \mathrm{O/C} < 0.8 \\ 0 & , 0.8 < \mathrm{O/C} \end{cases} \quad \text{(Eqn. 4)}$$

We suggest that the sigmoidal fit is more robust given its value at extremely low O/C values (< 0.2). Comparing to the second-order polynomial fit, the sigmoidal fit is chemically more reasonable at low O/C ratios with the predicted SRH value approaching 100%.

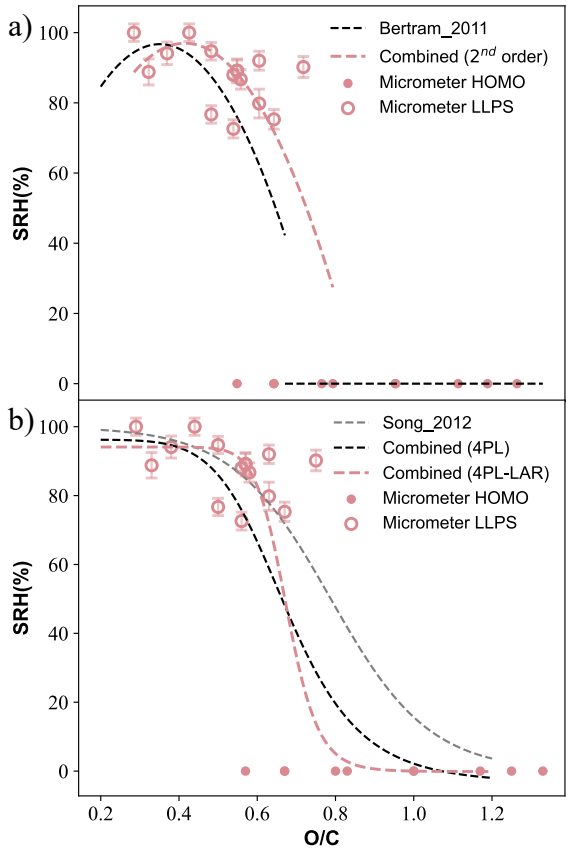

Figure 1. *The separation relative humidity (SRH) of aerosol particles containing organic compounds and ammonium sulfate (organic-to-inorganic mass ratio = 2:1). The open red circles are the updated dataset of SRH for micrometer-sized droplets composed of ternary systems, and the small red dots represent homogeneous aerosol particles (denoted by HOMO in the legend) that do not undergo LLPS (see detailed dataset information in Table S3). The dashed red lines in both a) and b) show the updated parameterization of the combined dataset for ternary systems from data by Bertram et al (2011),[12] Song et al. (2013),[35] and Bertram et al (2013)[12]. a) Polynomial fit following Bertram et al. (2011).[12] The black dashed lines denote the parameterizations for micrometer-sized aerosol particles by Bertram et al. (2011).[12] b) Sigmoidal fits using a four parameter logistic function (4PL, black dashed line) and a four-parameter logistic fit with the least absolute residuals robust fitting method (4PL-LAR, red dashed line). The grey dashed lines denotes the parameterizations for micrometer-sized aerosol particles by Song et al. (2012).[13]*

The SRH of Submicron Organic/AS Particles. We selected nine organic compounds with a range of O/C ratios that represent atmospheric secondary organic aerosol components with various functional groups and chemical structures (Table 1). At relatively high O/C ratios (O/C ≥ 0.56), we picked two to three organic species with different molecular structures to investigate the effect of molecular structure on submicron aerosol LLPS. The SRH of submicron aerosol particles are characterized using the onset SRH, the final SRH, and the mean SRH. The onset SRH refers to the RH value at which LLPS was observed for at least one aerosol particle during dehumidification experiments. The final SRH denotes the highest RH value at which all imaged aerosol particles with a sufficiently large diameter are phase separated. Note that aerosol particles that are sufficiently small (dry diameter smaller than 30nm) do not undergo LLPS.[31,33,39] The mean SRH is the average of all phase-separated aerosol particles between the onset SRH and final SRH. For example, the onset SRH of 2,5-hexanediol is 78%, the final SRH is 52%, and the mean SRH is 64±6% (Figure 2a). The morphologies of the submicron organic/AS particles are characterized from TEM images (Figure S1). A detailed description can be found in our previous work.[31,33,39] In brief, aerosol particles that undergo LLPS exhibit an inner phase boundary with different image contrast (and associated refractive indices) inside and outside the inner boundary, whereas homogeneous aerosol particles show no inner phase boundary. The measured data are shown in Figure 2 and summarized in Table 1. The effect of molecular structure for organic compounds with the same O/C ratio is discussed in the SI Section S3. The quantitative relationship between the measured

SRH values and different parameterization variables will be discussed in the following section.

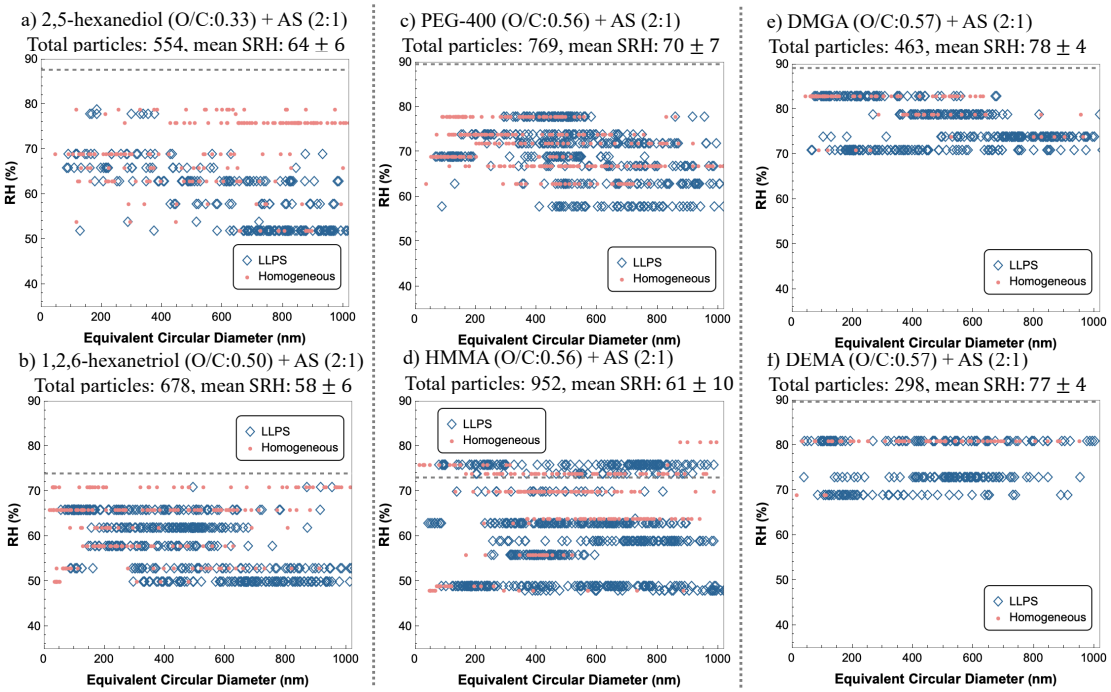

Figure 2. *Summary of LLPS (blue diamonds) vs. homogeneous mixing (red dots) in organic/AS particles with $mf_d(AS)$ values at 0.33 (organic:inorganic dry mass ratio = 2:1). a) 2,5-hexanediol; b) 1,2,6-hexaneteriol; c) polyethylene glycol (PEG-400); d) DL-4-hydroxy-3-methoxymandelic acid (HMMA); e) 3,3-dimethylglutaric acid (DMGA); f) diethyl malonic acid (DEMA). Particles were characterized at different RHs to determine whether they exhibit a homogeneous or phase-separated morphology. The gray dashed line represents the SRH of micrometer-sized droplets measured via optical microscopy. Each marker represents a single particle. All data points were collected at 298 K.*

The Parameterization of SRH for Submicron Organic/AS Particles. The variation in SRH between different organic/AS aerosol particles illustrates the complex effect of molecular structure on SRH. To account for the variability in SRH between different organic compounds, parameterization methods based on different chemical variables were evaluated to optimize the prediction of SRH. Herein, we fit the SRH for both micrometer and submicron aerosols with different variables that represent different aspects of molecular properties. The SRH values for micrometer droplets are

identical to those in Figure 1, while the submicron aerosol SRH values include six components measured in this study (Figure 2) and 2MGA-AS aerosols from our previous study.[33] Ideally, a parameterization method should fulfill the following criteria: i) the independent variable of the parameterization is reasonable from the perspective of physical chemistry; ii) the variable can differentiate the threshold for the occurrence of LLPS; iii) the method can fit the experimental data and predict the SRH sufficiently accurately for both micrometer and submicron sized aerosol particles; and iv) the method can bridge the differences between the SRH values for submicron aerosol and micrometer-sized droplets.

Following these criteria, we elected variables to represent the organic molecules that may reflect the affinity of the organic compounds to inorganic-rich or organic-rich phases: O/C ratio, LogP, LogD, LogS, molar mass, and the polarizability of the organic compounds. The O/C ratio is presented in the main text, as it has been most commonly used in the literature, and the other variables are presented in the SI section S5. As the scattering of the O/C ratio data suggest a threshold value (Figure 3), a four-parameter logistic function (4PL) was used for O/C ratios. All other results are displayed in Figures S5 – S8. The fitted functions and R^2 values are listed in Tables S4 – S7. The parameterization function should exhibit a threshold value that can differentiate the homogeneous and LLPS morphology: below the threshold, the corresponding organic aerosol particles do not undergo LLPS, whereas the functional form of SRH can be determined above the threshold. Although there are some outliers

at O/C ratios below 0.8, the O/C ratio can distinguish between a homogeneous morphology and LLPS, with a threshold value of 0.8.

For micrometer-sized droplets, the O/C ratio with 4PL-LAR fit showed the highest R^2 value of 0.85, whereas for other choices of the independent variable, the R^2 values are lower (0.22 for LogP, 0.29 for LogD, 0.04 for LogS, 0.77 for molar mass, and 0.54 for polarizability; see Tables S4 & S6). Using the O/C ratios and SRH values reported in field campaigns and flow tube studies, we predicted the SRH using the fitted 4PL-LAR model. The results were generally consistent, with discrepancies arising from the complex inorganic salt composition and size differences (Table S8, details discussed in SI Section S7).[42–44] This further highlights the importance of extending predictions to submicron aerosol particles.

For submicron particles, the R^2 value of all considered variables, except for the sigmoidal fit using O/C ratios (0.83) and the second-order fit using LogP (0.74), are low (< 0.4, Table S5 & S7). Fits to variables besides the O/C ratio are discussed in the SI. The variation in fits to SRH, especially for submicron aerosol particles, are large no matter which parametrization variable is selected. We also note that the dataset is limited, especially for the sigmoidal fits for O/C ratio, SRH data is absent in the downward sloping region, which can cause inaccuracy in the fitting. Therefore, we show that the O/C ratio showed correlation with SRH and can to some extent distinguish aerosol morphology. Additionally, as discussed in the SI, polarizability can distinguish aerosol morphology, and LogP showed a meaningful correlation with submicron aerosol SRH; therefore, other variables merit future investigation.

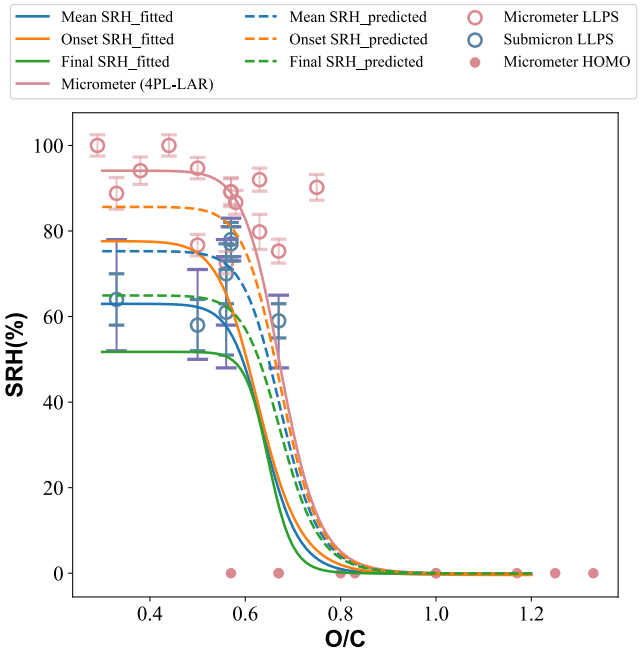

Figure 3. *Parameterizations of LLPS based on O/C ratio using sigmoidal fitting with a four-parameter logistic function. The solid red line denotes the parameterization of micrometer-sized droplets. The orange, blue and green colors represent the parameterization of the onset SRH, mean SRH, and final SRH, respectively. The solid lines denote the fitted results. The dashed lines are the results from the estimated scaling factors. The red marker represents the micrometer droplet SRH and the error bar represents the standard deviation. The blue marker represents the mean SRH of a given organic/AS submicron aerosol system, and the blue error bars denote the standard deviations. The purple error bars refer to the onset and final SRH, with the upper cap denoting the onset SRH and the lower cap denoting the final SRH. HOMO in the legend stands for homogeneous aerosol particles.*

As discussed above, when fitting the SRH of micrometer-sized droplets and submicron aerosol particles independently, we achieved different sets of coefficients for polynomial and sigmoidal functions. The fact that each dataset has its specific fit is hard to apply in practice, as the fitted coefficients and polynomial orders are highly dependent on the dataset, and the use of numerous functions can complicate the application of the parameterization. Therefore, for complex systems such as atmospheric aerosol particles, except for distinguishing the threshold and accurately fitting the SRH, the parametrization methods should be practical, and the independent

variable used should be easy to measure and effectively predict LLPS. We therefore designed a scaling factor that can relate the SRH of submicron aerosol particles to that of micrometer-sized droplets. Since the O/C ratio provided the best correlation with the SRH of micrometer droplets, we used a scaling factor based on the fit that uses O/C as the independent variable. By dividing the onset SRH, the mean SRH, and the final SRH of submicron aerosols by the mean SRH of micrometer droplets, respectively, we found that the calculated ratios have similar values across all organic/AS/water ternary systems investigated herein. We therefore defined the scaling factor (SF) for the onset SRH, the mean SRH, and the final SRH of submicron aerosol particles as a mean ratio of all $SRH(nano)_{onset}/SRH(micro)$, $SRH(nano)_{mean}/SRH(micro)$, $SRH(nano)_{final}/SRH(micro)$ values collected in this study. The SRH(micro) is the mean SRH value of micrometer droplets of each organic/AS mixture. We have illustrated that the standard deviation of the measured droplet SRH is low, and the measurement results are highly consistent across experiments. Figure 4 shows the calculated ratios as a function of the O/C ratio. Plots for LogP, molar mass, and polarizability are included in Figure S9. Given its definition, all of the scaling factors achieved are universal for all variables. The fluctuations of the data points around the fitted scaling factor are depicted in residual plots (Figure S10). The scaling factor for the onset SRH of submicron aerosols, SF_{onset} is 0.91. The scaling factor for the mean SRH of submicron aerosols, SF_{mean} is 0.80. The scaling factor for the final SRH of submicron aerosols, SF_{final} is 0.69. Given the distribution of the calculated ratios around the scaling factors, we

acknowledge that fundamentally each individual organic/AS system may have its own degree of suppression of SRH of submicron aerosols compared to the SRH of micrometer droplets. Herein, we established an empirical parameterization by assuming a uniform suppression effect that is independent of the components of the aerosol particles. However, future studies are needed to explore the underlying effects of various organic structures over a broad range of molar masses and functionalization degrees to achieve an accurate prediction of aerosol SRH on the basis of molecular structure.

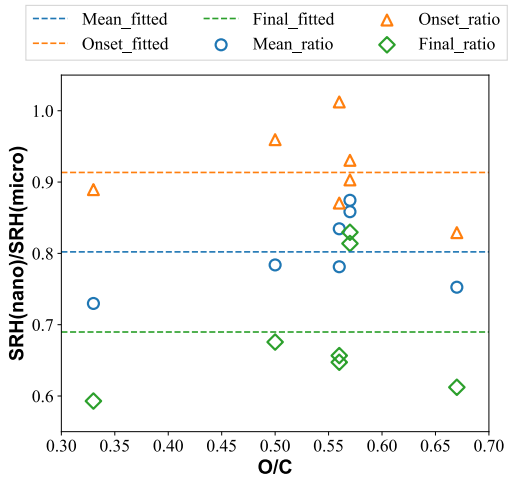

Figure 4. *The estimated value of the scaling factor (SF) using the collected submicron aerosol SRH and the micrometer-sized droplet SRH. The scattered points show the data distribution around the SF values for the O/C ratio. The orange, blue and green dashed lines represent the average SF for the onset SRH, mean SRH, and final SRH, respectively.* $SF_{onset} = 0.91$ *(orange),* $SF_{mean} = 0.80$ *(blue),* $SF_{final} = 0.69$ *(green).*

After determining the scaling factors, we applied the scaling factors to the fitted curves for micrometer-sized droplets, thereby predicting the expected corresponding SRH for submicron-sized particles. As shown in Figure 3, the orange dashed lines are the scaled onset SRH, the blue dash lines are the scaled mean SRH, and the green dash lines are the scaled final SRH. The predicted SRH of submicron aerosols are

compared with experimental data in Figure 5. The blue points denote the comparison between the experimental SRH for submicron aerosol particles and the predicated SRH for submicron aerosol particles that was scaled from the SRH for micrometer droplets. The prediction of SRH using the scaling factor showed a significant correlation with the experimental measurements (R^2=0.69). The shaded blue area denotes the 95% confidence region. We also calculated the region of uncertainty using the SF_{onset} for onset SRH and SF_{final} for the final SRH, and the region largely coincides with the 95% confidence region. Submicron aerosol SRH predicted using the scaling factors and the fitted functions for micrometer droplets based on all tested variables (O/C ratio, LogP, LogS, LogD, molar mass, and polarizability) are also evaluated in Figure 5. Even though the fitted parameterizations for most input variables showed weak correlation with micrometer droplet SRH, most of the predicted values for all variables lie in the 95% confidence region of the fit to the experimental data. The results above indicate that the effect of aerosol size on SRH can be effectively predicted using scaling factors, and the SF_{onset} and SF_{final} can characterize the uncertainty of the SF prediction. The distribution of the predicted SRH values in Figure 5 also suggests that the application of the scaling factor is not sensitive to the parameterization, as most of the predicted SRH values from different parametrizations lie in the uncertainty region established by the predicted onset and final SRH. Thus, the scaling factor and the parametrization method can be optimized independently with more experimental data, and the scaling factor for the size effect

can always be applied to the updated parameterization methods for micrometer droplets.

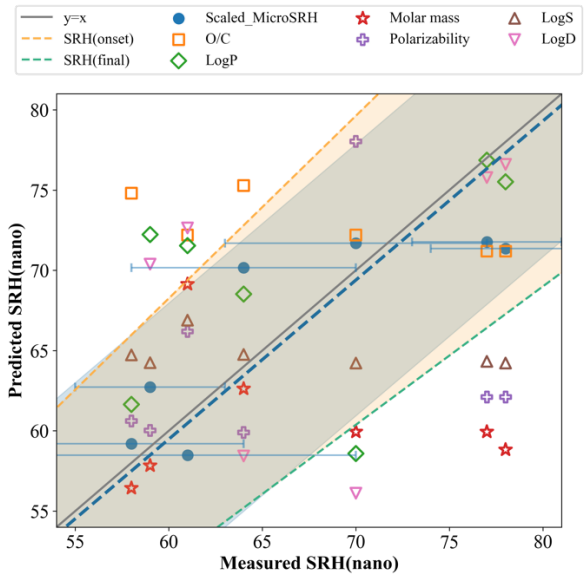

Figure 5. *SRH prediction of submicron-sized particles (y-axis) compared to direct measurements of submicron aerosol SRH (x-axis). The blue solid circles indicate submicron SRH predictions derived from micrometer droplet SRH measurements using the scaling factor (labelled as Scaled_MicroSRH). The open markers represent the predicted submicron aerosol SRH obtained through the combined parameterization of various fitted functions for micrometer droplet SRH and the scaling factor. The predictions are labelled based on the variables used for micrometer SRH fits: O/C ratio (sigmoidal fit, orange squares), LogP (polynomial fit, green diamonds), molar mass (polynomial fit, red stars), polarizability (polynomial fit, purple crosses), LogS (polynomial fit, brown upward triangles), and LogD (polynomial fit, pink downward triangles). The black line represents the identity line (y=x), and the blue dashed line shows the fit using the predicted Scaled_MicroSRH and the Measured SRH (nano) for submicron aerosol particles. The grey shaded area denotes the 95% confidence region of the linear fit (blue dashed line). The orange shaded area represents the region between the onset SRH (orange dashed line) and final SRH (green dashed line) predicted using the SF_{onset} and SF_{final}. Error bars represent the standard deviations of the Measured SRH (nano) values. Since all points at the same Measured SRH (nano) share identical error bars, only the error bar for the blue solid circles is shown.*

In our recent studies, we observed that for 2MGA-AS aerosols, the submicron aerosol SRH converged with that of micrometer-sized droplets after 60 min equilibration time, indicating a relatively slow, kinetically driven effect on the

suppressed SRH in submicron aerosol particles.[33] Therefore, combining the size effect and time evolution, we can depict the scaling factor for submicron aerosol SRH as a function of aerosol diameter (D) and equilibration time (t): $SRH_{nano} = SRH_{micro} \times SF(D,t)$, where

$$SF(D,t) = \delta(D) \cdot f(t)$$

$$\delta(D) = \begin{cases} 0, & D \leq 30\ nm \\ 1, & D > 30\ nm \end{cases}$$

$$f(t) = \begin{cases} SF, & t = 20\ min \\ 1, & t \geq 60\ min \end{cases}$$

This expression indicates that: i) aerosol particles < 30 nm wet diameter remain homogeneous regardless of the equilibration time (in this equation, this corresponds to $SRH_{nano} = 0$); ii) aerosol particles > 30 nm and with equilibration time = 20 min have a scaling factor equal to the ones determined in this study ($SF_{mean} = 0.80$, $SF_{onset} = 0.91$, $SF_{final} = 0.69$); iii) when aerosol particle diameter > 30 nm, and the equilibration time ≥ 60 min, the $SRH_{nano} = SRH_{micro}$. In addition, the uncertainty can be estimated using the SF_{onset} and SF_{final}. We note that an equilibration time of 60 minutes may not be the shortest time required for reaching the equivalence $SRH_{nano} = SRH_{micro}$, and future experiments are needed to find the accurate threshold time. Once the threshold equilibration time is confirmed, one can use that equilibration time to substitute the 60 min in the current SF function. We also note that the scaling factors are adequate for the equilibration time used herein (20 min) and may vary based on the equilibration time for $t < 20$ min and $20 < t < 60$ min. Our previous studies have shown that the 20 min SRH is overall representative for 20 to 30 min equilibration

time,[33] but additional characterization is needed to determine the range of scaling factors for different equilibration times.

Environmental Implications. Using the SRH measured for a wide variety of submicron organic/AS aerosol particles, we determined a parameterization for the SRH of submicron organic/inorganic aerosol particles as a function of several different variables describing the chemistry of the organic compound. According to our evaluation, the use of a scaling factor (SF) applied to the SRH parameterization of micrometer droplets can effectively estimate the SRH of submicron aerosol particles. Compared to the interpolation of measured SRH using either polynomial or sigmoidal fits, the combination of SF_{mean}, SF_{onset}, and SF_{final} covers the variation of measured submicron aerosol SRH, indicating that the scaling factor model can predict the mean SRH and characterize the uncertainty for submicron aerosol SRH within reasonable bounds considering the applications of these parameterizations. Current parameterizations of SRH rely on experimental data of micrometer droplets and model predictions under thermodynamic equilibrium conditions. The scaling factor method effectively connects a parameterization targeting submicron secondary aerosol to the micrometer-droplet-based parameterization. The scaling factor method enables the independent optimization of the scaling factor and the parametrization of the SRH for micrometer droplets, respectively. In addition, the two parts can be directly combined once an optimization of either part is achieved in future studies. Note also that the cut-off size and equilibration time are both incorporated into the scaling factor expression, as the size distribution and time evolution are significant

aspects of phase separation. Using the scaling factor established in this study along with future optimizations for the chemical composition (e.g., O/C ratios, polarizability etc.) of organic/inorganic aerosol particles, one can estimate the SRH for submicron aerosol particles based on a given aerosol size distribution, the period of time under stable conditions, and chemical composition.

In the meantime, we are aware of limitations of the current parameterization methods for atmospheric aerosol LLPS. The size effect in our scaling factor merely incorporates a cut-off size for the inhibition of submicron aerosol LLPS, as size dependence between SRH and aerosol diameter is not yet observed with the collected dataset. However, a more finely resolved size-dependent parameterization requires future studies with more size-resolved measurements. In addition to size-resolved experimental data, model predictions based on size-dependent thermodynamic models accounting for interfacial tension effects on LLPS may also aid in determining consistent size-dependence relationships for use in simpler parameterizations.[45,46]

For the LLPS dependence on aerosol composition, both inorganic and organic components play critical roles. We acknowledge that this study, along with the majority of literature studies, uses ammonium sulfate as the inorganic salt. Previous studies have shown that variations in inorganic components can significantly impact SRH.[14,43,47] However, while developing parameterizations for different inorganic salts is essential, it is currently not feasible due to the limited data available on this topic. Regarding organic components, among the investigated variables in this study, the O/C ratio showed the best fit in estimating the SRH for micrometer droplets and in

discerning the homogeneous and LLPS morphologies. Other independent variables, such as polarizability, molar mass, and LogP, may also be applicable. However, compared to O/C ratios and molar mass, parameters like polarizability and LogP, are not easily accessible from field measurements since their estimation requires molecular structure information (e.g., SMILES). For all tested variables, the correlation between the variables and submicron aerosol SRH is weak overall. This observation may be due to the combined effects of the chemical structure and the aerosol size effect. Taking the O/C ratio as an example, organic compounds with high O/C values may exhibit lower SRH in macroscopic systems yet tend to have a higher surface tension in aqueous droplets. In submicron aerosol particles, the higher surface tension can cause a stronger Kelvin effect, indicating a higher supersaturation (i.e., RH) for LLPS to occur.[46,48] Conversely, organic compounds with lower O/C ratios would have a higher SRH for micrometer droplets but a smaller Kelvin effect due to lower surface tension. Such effects may lead to a dampening in the SRH-dependence on the O/C ratio, especially for sub-100 nm droplets. Additionally, our previous work has also shown an effect of aerosol pH on LLPS; thus, the proton activity may need to be incorporated into future parameterizations.[27] Therefore, advances in practical parameterization methods that account for the protonation/deprotonation of functional groups in organic/inorganic aerosol particles are still needed. In the atmosphere, the gas-particle partitioning of aerosol particles, dictated by component volatility, is a key process influencing the evolution of aerosol phase state, particularly for aerosol particles containing highly volatile primary organic species. Future studies should

further explore the role of volatility as a parameter in LLPS for primary organic aerosols.

For atmospheric modeling and the evolution of organic/inorganic aerosol phase state, the aerosol size, composition, and ambient conditions may constantly change over time. Thus, the coupling between the dynamic change of the physical properties of atmospheric secondary aerosol particles and the scaling factor measured in this study ($SF(D,t)$) requires further investigation. Moreover, applying the relationship between the scaling factor and equilibration time to real atmospheric conditions require consideration of the timescales of other physical and chemical processes (e.g., deposition, chemical reactions). Ultimately, the interplay between these characteristic timescales will determine how the scaling factor should be applied in real atmospheric scenarios.

This study shows that a parameterization based on chemical composition ($f(Chem)$) demands further optimization due to the weak correlation between the investigated variables (O/C ratio, molar mass, LogP, LogS, and polarizability) and aerosol SRH (both micrometer-sized and submicron). In the meantime, we have shown that the scaling factor that depends on aerosol particle diameter and equilibration time ($SF(D,t)$) is a promising parameterization for all proxy atmospheric secondary aerosol particles studied here, which can be incorporated with an accurate chemistry-based parametrization framework ($f(Chem)$). Both the scaling factor and the chemistry-based parametrization can be optimized independently with an enlarged dataset, and can be directly combined together during application. Such a

parameterization method can be expressed as $SRH = f(Chem) \cdot SF(D, t)$. This form of parametrization is simple to apply and can be easily updated to improve the accuracy of SRH prediction. Accurate prediction of atmospheric aerosol phase state, particularly the SRH, is significant in predicting the aerosol-related atmospheric chemical and physical processes (e.g., gas-particle partitioning and heterogeneous chemistry), which in turn impacts the climate, air quality, and human health.[45,49] An accurate parametrization framework to predict the SRH will effectively reduce the uncertainty in atmospheric modeling.[50]

Associated Content

Supporting information

The supporting information contains detailed information on the literature data, example TEM images of SOA proxies, AIOMFAC-LLE predictions of phase diagrams, and the details for the fitted parametrization of aerosol SRH (Figures S1–S10, Tables S1–S8).

Author Information

Corresponding authors:

Miriam Arak Freedman – *Department of Chemistry, The Pennsylvania State University, University Park, Pennsylvania 16802, United States; Department of Meteorology and Atmospheric Science, The Pennsylvania State University, University Park, Pennsylvania 16802, United States;* Email: maf43@psu.edu Phone: 814-867-4267

TOC Art

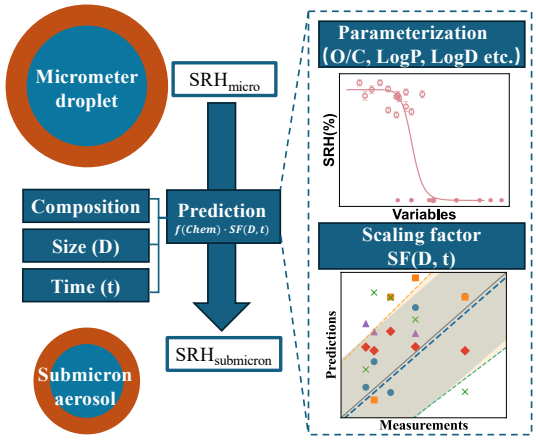

Authors

Qishen Huang –*Institute of Chemical Physics, School of Chemistry and Chemical Engineering, Beijing Institute of Technology, Beijing, 100081, China; Department of Chemistry, The Pennsylvania State University, University Park, Pennsylvania 16802, United States.*

Kiran R. Pitta - *Department of Chemistry, The Pennsylvania State University, University Park, Pennsylvania 16802, United States*

Andreas Zuend - *Department of Atmospheric and Oceanic Sciences, McGill University, Montreal, Quebec, H3A 0B9, Canada*

Notes

The authors declare no competing financial interest.

Acknowledgements

Q. H., K. R. P., and M. A. F. gratefully acknowledge the support from DOE grant DE-SC0018032. Q.H. acknowledges support by Beijing Municipal Natural Science Foundation (grant no. 8244070). A. Z. acknowledges support by the Natural Sciences and Engineering Research Council of Canada (grant no. RGPIN-2021-02688). We

thank the Materials Characterization Lab (MCL) at Penn State for the use of FEI Talos C TEM and the FEI Tecnai Lab6 TEM, and the Huck Institutes of the Life Sciences for the use of Gatan cryo-holder. We acknowledge J. L. Gray and M. Hazen for their help with TEM imaging.

Reference

(1) IPCC. *Climate Change 2013: The Physical Science Basis*; Cambridge University Press, 2013.

(2) Seinfeld, J. H.; Pandis, S. N.; Noone, K. *Atmospheric Chemistry and Physics: From Air Pollution to Climate Change*, 3rd ed.; John Wiley & Sons: NJ, 2016.

(3) Freedman, M. A. Phase Separation in Organic Aerosol. *Chem. Soc. Rev.* **2017**, *46* (24), 7694–7705.

(4) Heal, M. R.; Kumar, P.; Harrison, R. M. Particles, Air Quality, Policy and Health. *Chem. Soc. Rev.* **2012**, *41* (19), 6606–6630.

(5) Freedman, M. A.; Huang, Q.; Pitta, K. R. Phase Transitions in Organic and Organic/Inorganic Aerosol Particles. *Annu. Rev. Phys. Chem.* **2024**, *75* (1), 257–281.

(6) Kanakidou, M.; Seinfeld, J. H.; Pandis, S. N.; Barnes, I.; Dentener, F. J.; Facchini, M. C.; Van Dingenen, R.; Ervens, B.; Nenes, A.; Nielsen, C. J.; Swietlicki, E.; Putaud, J. P.; Balkanski, Y.; Fuzzi, S.; Horth, J.; Moortgat, G. K.; Winterhalter, R.; Myhre, C. E. L.; Tsigaridis, K.; Vignati, E.; Stephanou, E. G.; Wilson, J. Organic Aerosol and Global Climate Modelling: A Review. *Atmos. Chem. Phys.* **2005**, *5* (4), 1053–1123.

(7) Xu, W.; Sun, Y.; Wang, Q.; Zhao, J.; Wang, J.; Ge, X.; Xie, C.; Zhou, W.; Du, W.; Li, J.; Fu, P.; Wang, Z.; Worsnop, D. R.; Coe, H. Changes in Aerosol Chemistry From 2014 to 2016 in Winter in Beijing: Insights From High-Resolution Aerosol Mass Spectrometry. *J. Geophys. Res. Atmos.* **2019**, *124* (2), 1132–1147.

(8) Nie, W.; Yan, C.; Huang, D. D.; Wang, Z.; Liu, Y.; Qiao, X.; Guo, Y.; Tian, L.; Zheng, P.; Xu, Z.; Li, Y.; Xu, Z.; Qi, X.; Sun, P.; Wang, J.; Zheng, F.; Li, X.; Yin, R.; Dallenbach, K. R.; Bianchi, F.; Petäjä, T.; Zhang, Y.; Wang, M.; Schervish, M.; Wang, S.; Qiao, L.; Wang, Q.; Zhou, M.; Wang, H.; Yu, C.; Yao, D.; Guo, H.; Ye, P.; Lee, S.; Li, Y. J.; Liu, Y.; Chi, X.; Kerminen, V. M.; Ehn, M.; Donahue, N. M.; Wang, T.; Huang, C.; Kulmala, M.; Worsnop, D.; Jiang, J.; Ding, A. Secondary Organic Aerosol Formed by Condensing Anthropogenic Vapours over China's Megacities. *Nat. Geosci.* **2022**, *15* (4), 255–261.

(9) Reid, J. P.; Bertram, A. K.; Topping, D. O.; Laskin, A.; Martin, S. T.; Petters, M. D.; Pope, F. D.; Rovelli, G. The Viscosity of Atmospherically Relevant Organic Particles. *Nat. Commun.* **2018**, *9* (1), 1–14.

(10) Zuend, A.; Marcolli, C.; Peter, T.; Seinfeld, J. H. Computation of Liquid-Liquid Equilibria and Phase Stabilities: Implications for RH-Dependent Gas/Particle Partitioning of Organic-Inorganic Aerosols. *Atmos. Chem. Phys.* **2010**, *10* (16),

7795–7820.

(11) Zhou, S.; Hwang, B. C. H.; Lakey, P. S. J.; Zuend, A.; Abbatt, J. P. D.; Shiraiwa, M. Multiphase Reactivity of Polycyclic Aromatic Hydrocarbons Is Driven by Phase Separation and Diffusion Limitations. *Proc. Natl. Acad. Sci. U. S. A.* **2019**, *116* (24), 11658–11663.

(12) Bertram, A. K.; Martin, S. T.; Hanna, S. J.; Smith, M. L.; Bodsworth, A.; Chen, Q.; Kuwata, M.; Liu, A.; You, Y.; Zorn, S. R. Predicting the Relative Humidities of Liquid-Liquid Phase Separation, Efflorescence, and Deliquescence of Mixed Particles of Ammonium Sulfate, Organic Material, and Water Using the Organic-to-Sulfate Mass Ratio of the Particle and the Oxygen-to-Carbon Ele. *Atmos. Chem. Phys.* **2011**, *11* (21), 10995–11006.

(13) Song, M.; Marcolli, C.; Krieger, U. K.; Zuend, A.; Peter, T. Liquid-Liquid Phase Separation in Aerosol Particles: Dependence on O:C, Organic Functionalities, and Compositional Complexity. *Geophys. Res. Lett.* **2012**, *39* (19), 1–5.

(14) You, Y.; Renbaum-Wolff, L.; Bertram, A. K. Liquid-Liquid Phase Separation in Particles Containing Organics Mixed with Ammonium Sulfate, Ammonium Bisulfate, Ammonium Nitrate or Sodium Chloride. *Atmos. Chem. Phys.* **2013**, *13* (23), 11723–11734.

(15) Huang, Y.; Mahrt, F.; Xu, S.; Shiraiwa, M.; Zuend, A.; Bertram, A. K. Coexistence of Three Liquid Phases in Individual Atmospheric Aerosol Particles. *Proc. Natl. Acad. Sci. U. S. A.* **2021**, *118* (16).

(16) Mahrt, F.; Huang, Y.; Zaks, J.; Devi, A.; Peng, L.; Ohno, P. E.; Qin, Y. M.; Martin, S. T.; Ammann, M.; Bertram, A. K. Phase Behavior of Internal Mixtures of Hydrocarbon-like Primary Organic Aerosol and Secondary Aerosol Based on Their Differences in Oxygen-to-Carbon Ratios. *Environ. Sci. Technol.* **2022**, *56* (7), 3960–3973.

(17) Mahrt, F.; Peng, L.; Zaks, J.; Huang, Y.; Ohno, P. E.; Smith, N. R.; Gregson, F. K. A.; Qin, Y.; Faiola, C. L.; Martin, S. T.; Nizkorodov, S. A.; Ammann, M.; Bertram, A. K. Not All Types of Secondary Organic Aerosol Mix: Two Phases Observed When Mixing Different Secondary Organic Aerosol Types. *Atmos. Chem. Phys.* **2022**, *22* (20), 13783–13796.

(18) Zuend, A.; Marcolli, C.; Luo, B. P.; Peter, T. *A Thermodynamic Model of Mixed Organic-Inorganic Aerosols to Predict Activity Coefficients*; 2008; Vol. 8. https://doi.org/10.5194/acp-8-4559-2008.

(19) Yin, H.; Dou, J.; Klein, L.; Krieger, U. K.; Bain, A.; Wallace, B. J.; Preston, T. C.; Zuend, A. Extension of the AIOMFAC Model by Iodine and Carbonate Species: Applications for Aerosol Acidity and Cloud Droplet Activation. *Atmos. Chem. Phys.* **2022**, *22* (2), 973–1013.

(20) Zuend, A.; Marcolli, C.; Booth, A. M.; Lienhard, D. M.; Soonsin, V.; Krieger, U. K.; Topping, D. O.; McFiggans, G.; Peter, T.; Seinfeld, J. H. New and Extended Parameterization of the Thermodynamic Model AIOMFAC: Calculation of Activity Coefficients for Organic-Inorganic Mixtures Containing Carboxyl, Hydroxyl, Carbonyl, Ether, Ester, Alkenyl, Alkyl, and Aromatic Functional Groups. *Atmos. Chem. Phys.* **2011**, *11* (17), 9155–9206.

(21) Zuend, A.; Seinfeld, J. H. A Practical Method for the Calculation of Liquid-Liquid Equilibria in Multicomponent Organic-Water-Electrolyte Systems Using Physicochemical Constraints. *Fluid Phase Equilib.* **2013**, *337*, 201–213.
(22) Altaf, M. B.; Zuend, A.; Freedman, M. A. Role of Nucleation Mechanism on the Size Dependent Morphology of Organic Aerosol. *Chem. Commun.* **2016**, *52* (59), 9220–9223.
(23) Pye, H. O. T.; Zuend, A.; Fry, J. L.; Isaacman-VanWertz, G.; Capps, S. L.; Appel, K. W.; Foroutan, H.; Xu, L.; Ng, N. L.; Goldstein, A. H. Coupling of Organic and Inorganic Aerosol Systems and the Effect on Gas-Particle Partitioning in the Southeastern US. *Atmos. Chem. Phys.* **2018**, *18* (1), 357–370.
(24) Losey, D. J.; Parker, R. G.; Freedman, M. A. PH Dependence of Liquid-Liquid Phase Separation in Organic Aerosol. *J. Phys. Chem. Lett.* **2016**, *7* (19), 3861–3865.
(25) Tong, Y.; Meng, X.; Zhou, B.; Sun, R.; Wu, Z.; Hu, M.; Ye, A. Detecting the PH-Dependent Liquid-Liquid Phase Separation of Single Levitated Aerosol Microdroplets via Laser Tweezers-Raman Spectroscopy. *Front. Phys.* **2022**, No. August, 1–8.
(26) Lei, Z.; Chen, Y.; Zhang, Y.; Cooke, M. E.; Ledsky, I. R.; Armstrong, N. C.; Olson, N. E.; Zhang, Z.; Gold, A.; Surratt, J. D.; Ault, A. P. Initial PH Governs Secondary Organic Aerosol Phase State and Morphology after Uptake of Isoprene Epoxydiols (IEPOX). *Environ. Sci. Technol.* **2022**, *56* (15), 10596–10607.
(27) Losey, D. J.; Ott, E. J. E.; Freedman, M. A. Effects of High Acidity on Phase Transitions of an Organic Aerosol. *J. Phys. Chem. A* **2018**, *122* (15), 3819–3828.
(28) Veghte, D. P.; Altaf, M. B.; Freedman, M. A. Size Dependence of the Structure of Organic Aerosol. *J. Am. Chem. Soc.* **2013**, *135* (43), 16046–16049.
(29) Kucinski, T. M.; Dawson, J. N.; Freedman, M. A. Size-Dependent Liquid-Liquid Phase Separation in Atmospherically Relevant Complex Systems. *J. Phys. Chem. Lett.* **2019**, *10* (21), 6915–6920.
(30) Altaf, M. B.; Freedman, M. A. Effect of Drying Rate on Aerosol Particle Morphology. *J. Phys. Chem. Lett.* **2017**, *8* (15), 3613–3618.
(31) Kucinski, T. M.; Ott, E. J. E.; Freedman, M. A. Dynamics of Liquid-Liquid Phase Separation in Submicrometer Aerosol. *J. Phys. Chem. A* **2021**, *125*, 41.
(32) Freedman, M. A. Liquid-Liquid Phase Separation in Supermicrometer and Submicrometer Aerosol Particles. *Acc. Chem. Res.* **2020**, *53* (6), 1102–1110.
(33) Huang, Q.; Pitta, K. R.; Constantini, K.; Ott, E. J. E.; Zuend, A.; Freedman, M. A. Experimental Phase Diagram and Its Temporal Evolution for Submicron 2-Methylglutaric Acid and Ammonium Sulfate Aerosol Particles. *Phys. Chem. Chem. Phys.* **2024**, *26* (4), 2887–2894.
(34) Ren, S.; Yao, L.; Wang, Y.; Yang, G.; Liu, Y.; Li, Y.; Lu, Y.; Wang, L.; Wang, L. Volatility Parameterization of Ambient Organic Aerosols at a Rural Site of the North China Plain. *Atmos. Chem. Phys.* **2022**, *22* (14), 9283–9297.
(35) Han, S.; Hong, J.; Luo, Q.; Xu, H.; Tan, H.; Wang, Q.; Tao, J.; Zhou, Y.; Peng, L.; He, Y.; Shi, J.; Ma, N.; Cheng, Y.; Su, H. Hygroscopicity of Organic

Compounds as a Function of Organic Functionality, Water Solubility, Molecular Weight, and Oxidation Level. *Atmos. Chem. Phys.* **2022**, *22* (6), 3985–4004.

(36) Dette, H. P.; Qi, M.; Schröder, D. C.; Godt, A.; Koop, T. Glass-Forming Properties of 3-Methylbutane-1,2,3-Tricarboxylic Acid and Its Mixtures with Water and Pinonic Acid. *J. Phys. Chem. A* **2014**, *118* (34), 7024–7033.

(37) Shiraiwa, M.; Li, Y.; Tsimpidi, A. P.; Karydis, V. A.; Berkemeier, T.; Pandis, S. N.; Lelieveld, J.; Koop, T.; Pöschl, U. Global Distribution of Particle Phase State in Atmospheric Secondary Organic Aerosols. *Nat. Commun.* **2017**, *8*, 1–7.

(38) Gorkowski, K.; Preston, T. C.; Zuend, A. Relative-Humidity-Dependent Organic Aerosol Thermodynamics via an Efficient Reduced-Complexity Model. *Atmos. Chem. Phys.* **2019**, *19* (21), 13383–13407.

(39) Kucinski, T. M.; Ott, E. J. E.; Freedman, M. A. Flash Freeze Flow Tube to Vitrify Aerosol Particles at Fixed Relative Humidity Values. *Anal. Chem.* **2020**, *92* (7), 5207–5213.

(40) Xiong, G.; Wu, Z.; Yi, J.; Fu, L.; Yang, Z.; Hsieh, C.; Yin, M.; Zeng, X.; Wu, C.; Lu, A.; Chen, X.; Hou, T.; Cao, D. ADMETlab 2.0: An Integrated Online Platform for Accurate and Comprehensive Predictions of ADMET Properties. *Nucleic Acids Res.* **2021**, *49* (W1), W5–W14.

(41) Song, M.; Marcolli, C.; Krieger, U. K.; Lienhard, D. M.; Peter, T. Morphologies of Mixed Organic/Inorganic/Aqueous Aerosol Droplets. *Faraday Discuss.* **2013**, *165*, 289–316.

(42) Smith, N. R.; Crescenzo, G. V.; Huang, Y.; Hettiyadura, A. P. S.; Siemens, K.; Li, Y.; Faiola, C. L.; Laskin, A.; Shiraiwa, M.; Bertram, A. K.; Nizkorodov, S. A. Viscosity and Liquid-Liquid Phase Separation in Healthy and Stressed Plant SOA. *Environ. Sci. Atmos.* **2021**, *1* (3), 140–153.

(43) Yao, M.; Zhao, Y.; Chang, C.; Wang, S.; Li, Z.; Li, C.; Chan, A. W. H.; Xiao, H. Multiphase Reactions between Organic Peroxides and Sulfur Dioxide in Internally Mixed Inorganic and Organic Particles: Key Roles of Particle Phase Separation and Acidity. *Environ. Sci. Technol.* **2023**, *57* (41), 15558–15570.

(44) Song, M.; Jeong, R.; Kim, D.; Qiu, Y.; Meng, X.; Wu, Z.; Zuend, A.; Ha, Y.; Kim, C.; Kim, H.; Gaikwad, S.; Jang, K. S.; Lee, J. Y.; Ahn, J. Comparison of Phase States of PM2.5over Megacities, Seoul and Beijing, and Their Implications on Particle Size Distribution. *Environ. Sci. Technol.* **2022**, *56* (24), 17581–17590.

(45) Schmedding, R.; Zuend, A. A Thermodynamic Framework for Bulk-Surface Partitioning in Finite-Volume Mixed Organic-Inorganic Aerosol Particles and Cloud Droplets. *Atmos. Chem. Phys.* **2023**, *23* (13), 7741–7765.

(46) Schmedding, R.; Zuend, A. The Role of Interfacial Tension in the Size-Dependent Phase Separation of Atmospheric Aerosol Particles. **2024**, No. July, 1–35.

(47) Ott, E.-J. E.; Kucinski, T. M.; Dawson, J. N.; Freedman, M. A. Use of Transmission Electron Microscopy for Analysis of Aerosol Particles and Strategies for Imaging Fragile Particles. *Anal. Chem.* **2021**, *93* (33), 11347–11356.

(48) Seinfeld, J. H.; Pandis, S. N. *Atmospheric Chemistry and Physics: From Air Pollution to Climate Change*, Third Edit.; John Wiley & Sons, 2016.

(49) Pye, H. O. T.; Murphy, B. N.; Xu, L.; Ng, N. L.; Carlton, A. G.; Guo, H.; Weber, R.; Vasilakos, P.; Wyat Appel, K.; Hapsari Budisulistiorini, S.; Surratt, J. D.; Nenes, A.; Hu, W.; Jimenez, J. L.; Isaacman-Vanwertz, G.; Misztal, P. K.; Goldstein, A. H. On the Implications of Aerosol Liquid Water and Phase Separation for Organic Aerosol Mass. *Atmos. Chem. Phys.* **2017**, *17* (1), 343–369.

(50) Yao, Y.; Curtis, J. H.; Ching, J.; Zheng, Z.; Riemer, N. Quantifying the Effects of Mixing State on Aerosol Optical Properties. *Atmos. Chem. Phys.* **2022**, *22* (14), 9265–9282.